flux for A = 1, 16, and 32 of 0.0046, 0.010, and 0.0240, respectively.
15. During its normal open-source (ions or neutrals) operation in the ionosphere and atmosphere of Titan, where the molecules are cold and the relative velocity is dominated by the spacecraft ram velocity, the entire distribution is within the instrument's compensation region volume (*10*), defined by the energy/velocity acceptance along the FOV and the velocity width perpendicular to this associated with the angular width of the FOV. However, during operations in the period after orbit insertion (over the A ring), only a small fraction of the ion distribution is captured in the compensation region.
16. The peak value of the distribution function, f, from INMS measurements for time periods when the compensation velocity is near the ring is the INMS density divided by the velocity space compensation volume (*10*). For H^+, O^+, and O_2^+, the peak f values are about 10^{-18} s^3/cm^6, 3×10^{-19} s^3/cm^6, and 10^{-18} s^3/cm^6, respectively.
17. D. A. Gurnett *et al.*, *Science* **307**, 1255 (2005).
18. The background rate of INMS in the csn mode has steadily diminished in the months after Saturn Orbit Insertion.
19. A. J. Kliore, D. P. Hinson, F. M. Flasar, A. F. Nagy, T. E. Cravens, *Science* **277**, 355 (1997).
20. W. F. Huebner, P. T. Giguere, *Astrophys. J.* **238**, 753 (1980).
21. Ions moving away from the ring plane along the magnetic field are reflected by the magnetic mirror formed by converging field lines and will return to the ring plane where they are removed from the plasma environment/ionosphere. This bounce time, T_{bounce}, is ≈3 hours and should also be the ion lifetime. However, because of a small northward offset of Saturn's magnetic dipole (*24*), some ions with very small vertical velocities might be trapped and have longer lifetimes.
22. A. J. Coates, *Geophys. Monogr. Am. Geophys. Union 61* (American Geophysical Union, Washington, DC, 1991), pp. 301–310.
23. J. G. Luhmann, in *Geophys. Monogr. Am. Geophys. Union 61* (American Geophysical Union, Washington, DC, 1991), pp. 5–16.
24. J. E. P. Connerney, L. Davis Jr., D. L. Chenette, in *Saturn*, T. Gehrels, M. S. Matthews, Eds. (Univ. of Arizona Press, Tucson, AZ, 1984), pp. 354–377.
25. We thank R. Johnson and F. Crary for useful and insightful discussions and comments. We are also very grateful for the hard work and dedication of our engineering, technical, and operational staff: G. Fletcher, E. Walter, R. Miller, J. Xu, J. Parajeko, D. Gell, and R. Thorpe. We thank D. Eddy, I. Robertson, and T. Hunt-Ward for technical help with the figures and text. Financial support from the NASA Cassini project is acknowledged.

28 September 2004; accepted 2 December 2004
10.1126/science.1105734

REPORT

Composition and Dynamics of Plasma in Saturn's Magnetosphere

D. T. Young,[1]* J.-J. Berthelier,[2] M. Blanc,[3] J. L. Burch,[1] S. Bolton,[4] A. J. Coates,[5] F. J. Crary,[1] R. Goldstein,[1] M. Grande,[6] T. W. Hill,[7] R. E. Johnson,[8] R. A. Baragiola,[8] V. Kelha,[9] D. J. McComas,[1] K. Mursula,[10] E. C. Sittler,[11] K. R. Svenes,[12] K. Szegö,[13] P. Tanskanen,[10] M. F. Thomsen,[14] S. Bakshi,[11] B. L. Barraclough,[14] Z. Bebesi,[13] D. Delapp,[14] M. W. Dunlop,[6] J. T. Gosling,[14] J. D. Furman,[1] L. K. Gilbert,[5] D. Glenn,[11] C. Holmlund,[9] J.-M. Illiano,[2] G. R. Lewis,[5] D. R. Linder,[5] S. Maurice,[3] H. J. McAndrews,[5] B. T. Narheim,[12] E. Pallier,[3] D. Reisenfeld,[14,15] A. M. Rymer,[5] H. T. Smith,[8] R. L. Tokar,[14] J. Vilppola,[10] C. Zinsmeyer[1]

During Cassini's initial orbit, we observed a dynamic magnetosphere composed primarily of a complex mixture of water-derived atomic and molecular ions. We have identified four distinct regions characterized by differences in both bulk plasma properties and ion composition. Protons are the dominant species outside about 9 R_S (where R_S is the radial distance from the center of Saturn), whereas inside, the plasma consists primarily of a corotating comet-like mix of water-derived ions with ~3% N^+. Over the A and B rings, we found an ionosphere in which O_2^+ and O^+ are dominant, which suggests the possible existence of a layer of O_2 gas similar to the atmospheres of Europa and Ganymede.

Most of what was known about Saturn's magnetosphere before Cassini's arrival was derived from the Pioneer 11 and Voyager 1 and 2 encounters from 1979 to 1981 (*1–5*) and from models based on that data (*6–8*). The measurements reported here were made with the Cassini plasma spectrometer (CAPS) (*9–11*) during the initial passage of the Cassini spacecraft through the near-equatorial regions of Saturn's magnetosphere. The CAPS instrument is made up of three plasma sensors.The first is the ion mass spectrometer (IMS), which measures ion energy per charge (E/Q) between 1 V and 50 kV with a resolution of $\Delta E/E = 0.17$. It simultaneously measures ion mass per charge (M/Q) from 1 to ~100 atomic mass units (amu) per charge, e, with a mass resolution $M/\Delta M \approx 60$. The second sensor is the electron spectrometer (ELS), which measures electron energy from 0.6 eV to 28 keV with $\Delta E/E$ = 0.17. The IMS and ELS are able to detect ion and electron densities as low as ~10^3 m^{-3}. The third sensor is the ion beam spectrometer (IBS), which measures ion E/Q with a very high resolution of $\Delta E/E = 0.017$, which is appropriate for narrowly beamed distributions.

The energy-time spectrogram (Fig. 1) and bulk plasma parameters (Fig. 2) give a broad overview of structures and events found 24 hours on either side of Cassini's closest approach to Saturn [02:39 universal time (UT) on 1 July 2004]. Within this time period on both inbound and outbound trajectories, we observed four regions with different physical and chemical characteristics: (i) The outer, or high-latitude, magnetosphere contains tenuous hot plasma dominated by H^+. (ii) A region we term the outer plasmasphere consists of highly variable, partially corotating plasma that contains a mixture of H^+, O^+, and water-group ions (denoted as W^+ and defined as a combination of OH^+, H_2O^+, and H_3O^+). (iii) The inner plasmasphere is less variable and closer to rigid corotation than the outer plasmasphere, and is made up primarily of O^+ and W^+. (iv) A layer of plasma consisting of O^+ and O_2^+ is located directly over the A and B rings. The boundaries separating these four regions are distinguished by changes not only in bulk plasma properties but also in chemical composition.

On the spacecraft's inbound trajectory, Saturn's magnetopause crossed over the spacecraft nine times between 34.6 and 30.6 R_S (1 R_S = 60,330 km). Just inside the magnetopause, plasma densities fell below the detection limits of the IMS. In particular, N^+, which might have been expected in the region of Titan's orbit (20.25 R_S), was not detected on either the inbound or outbound legs, possibly because the spacecraft was

[1]Southwest Research Institute, San Antonio, TX 78238, USA. [2]Centre d'Etude des Environnements Terrestre et Planétaires, Observatoire de St. Maur, 94107 St. Maur, France. [3]Observatoire Midi-Pyrenées, 31400 Toulouse, France. [4]Jet Propulsion Laboratory, Pasadena, CA 91109, USA. [5]University College London, Mullard Space Science Laboratory, Holmbury Saint Mary, Dorking, Surrey RH5 6NT, UK. [6]Rutherford Appleton Laboratory, Chilton, Didcot, Oxfordshire OX11 0QX, UK. [7]Department of Physics and Astronomy, Rice University, Houston, TX 77251, USA. [8]Engineering Physics, University of Virginia, Charlottesville, VA 22904, USA. [9]VTT Industrial Systems, 02044, Finland. [10]Department of Physical Sciences, University of Oulu, 90014 Oulu, Finland. [11]Goddard Space Flight Center, Greenbelt, MD 20771, USA. [12]Division for Electronics, Norwegian Defense Research Establishment, N-2027 Kjeller, Norway. [13]KFKI Research Institute for Particle and Nuclear Physics, H-1525 Budapest, Hungary. [14]Space and Atmospheric Science Group, Los Alamos National Laboratory, Los Alamos, NM 87545, USA. [15]Department of Physics and Astronomy, University of Montana, Missoula, MT 59812, USA.

*To whom correspondence should be addressed. E-mail: dyoung@swri.edu

several ion-scale heights distant from Titan's orbital plane (*12*). At 14.4 R_S inbound and 13.6 R_S outbound (A and A′ in Figs. 1 and 2), Cassini crossed a ~0.2-R_S-thick boundary identifiable by an order-of-magnitude increase in density (from $\sim 3 \times 10^4$ to $\sim 3 \times 10^5$ m^{-3}). The density increase enabled us to establish that approximate plasma corotation occurs inside this boundary. Corotation is indicated by the broad peaks in count rates (Fig. 1) centered on the corotation energy (*13*) of protons and/or water-group ions. The A and A′ boundaries can be interpreted as a plasmapause, a structure that, at Earth, represents the last closed equipotential of plasma flow around the planet (*14*). At Saturn, however, magnetic flux tubes beyond the plasmapause are relatively empty because their **E** × **B** (where **E** and **B** are the planetary electric and magnetic fields, respectively) drift paths carry them through the magnetotail where centrifugal force can cause them to break open, spilling plasma down the tail (*15*).

Near ~9 R_S inbound and ~7.6 R_S outbound, Cassini crossed a second boundary (B and B′ in Figs. 1 and 2, B in Fig. 3) and moved into a region we identify as the inner plasmasphere. Here, ion motion is still organized by corotation. However, because the total ion energy is the sum of corotational and thermal energies, the bulk of the distribution appears above the theoretical corotation velocity curves in Figs. 1 and 2. A second characteristic of the inner plasmasphere is that the electron data are best fit by a bi-Maxwellian velocity distribution that yields separate densities and temperatures for two components. The colder component (~3 to 30 eV) increases in density and decreases in temperature with decreasing radial distance (Fig. 2). The hotter component (~100 to 1000 eV) has the opposite behavior; it decreases in density and increases in temperature with decreasing radial distance. Inside 6.3 R_S inbound (5.9 R_S outbound), the cold electron component is bounded by the proton corotation energy, a phenomenon that has yet to be explained (Fig. 1). Coincident with the change in bulk plasma characteristics in the inner plasmasphere is a change in ion composition. The abundance of O^+ and W^+ relative to protons increases sharply at the B boundary (Fig. 3) by more than an order of magnitude, reaching ratios greater than unity (because of pointing restrictions, there is no corresponding composition data outbound). Because the spacecraft is within ~1 ion-scale height of the equatorial plane, the change in composition must be caused by a radial gradient and not by scale-height effects. Neither the low relative abundance of O^+ and W^+ outside 9 R_S nor the steepness of the composition gradient agrees with Voyager observations (*6*, *16*) or with existing plasma generation models (*8*, *17*). These

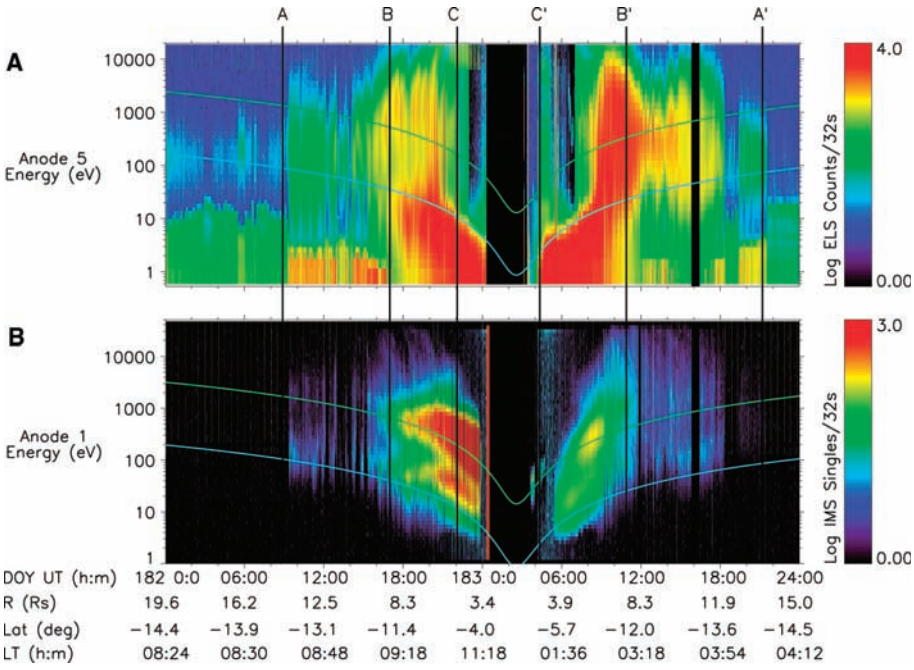

Fig. 1. An energy-time spectrogram showing particle counting rates (proportional to energy flux) in Saturn's magnetosphere for 30 June to 1 July 2004 (DOY 182 and 183). Data are averaged over 32 s. The color bars at right indicate rate intensity on a log scale. (**A**) Electron counting rates and (**B**) ion counting rates are shown. Energy increases along the vertical axes. Anodes 5 and 1 refer to the parts of the ELS and IMS detectors, respectively, that were most sensitive to electron and ion distributions over this period. The asymmetry in ion counting rates before and after closest approach (02:39 UT) is caused in part by a change in spacecraft pointing relative to the corotational flow direction. Universal time (UT), radial distance from the center of Saturn in R_S, latitude (Lat), and local time (LT) with respect to Saturn are shown on the horizontal axis. The curved lines superimposed on the plots give the energy corresponding to the theoretical corotation velocity (*13*) for O^+ (upper curve in both panels) and H^+ (lower curve). The data have been corrected for penetrating radiation background. Vertical black lines labeled A, B, and C indicate plasma boundaries on the inbound trajectory, whereas A′, B′, and C′ are the corresponding boundaries on the outbound leg. CAPS was turned off in the interval 00:00 to 03:25 UT on 1 July during the Cassini main engine burn.

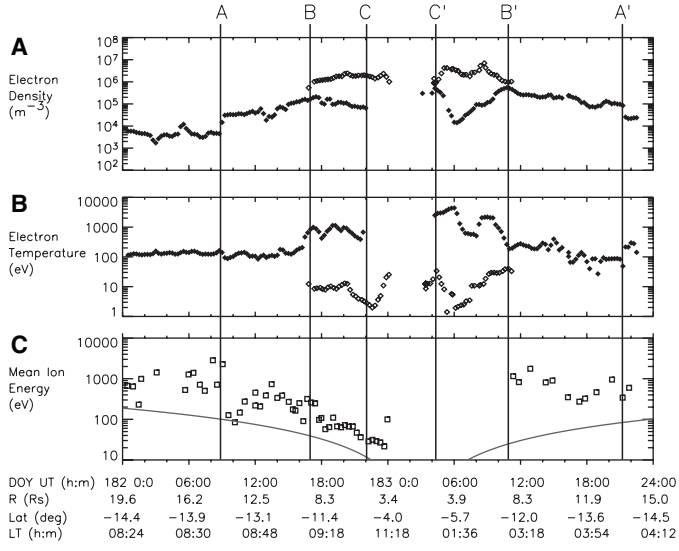

Fig. 2. Profiles of plasma parameters determined from moments of the electron and ion distributions. (**A**) Electron density. Solid symbols are the hot electron population. Open symbols are the cold electron population. The calculation of density is based on a fit to the electron distribution function assuming an isotropic bi-Maxwellian distribution of speeds in the spacecraft frame of reference. The two distributions become distinct and are well fit as a bi-Maxwellian only in the inner plasmasphere defined as the region between the B–C and B′–C′ boundaries. When the spacecraft is negatively charged, this density only includes the fraction of electrons with energies above the spacecraft potential. (**B**) Electron temperature derived in the same way as the densities shown in (A). (**C**) Proton mean kinetic energy is the statistical average energy of all observed protons and includes both the energy caused by the corotation of the plasma and thermal energy of the particles. On the outbound leg, poor spacecraft pointing relative to the corotational flow compromised the ion moment calculations. The curved line corresponds to the proton corotational energy.

results, although preliminary, could be attributable to changes in Saturn's magnetosphere after Voyager's observations or to differences in measurement methods.

Inside ~10 R_S, and as close as 4.4 R_S to Saturn, time-dispersed signatures of ions and electrons arriving at the spacecraft suggest that, at times, we are observing fresh plasma being injected deeper into the magnetosphere. Many of these features, which are too short to be visible at the scale of Fig. 1, are characterized by the initial arrival of high-energy ions (~10 keV) followed by the arrival of progressively lower energies, and then the appearance of low-energy electrons followed by progressively higher energies. Similar structures occur quite commonly at Earth (*18*) and have been observed at Jupiter (*19*), but have not previously been reported at Saturn. At Earth, the injections are caused by sudden increases in the global convection electric field. For rapidly rotating planets like Jupiter and Saturn, injections can be explained as centrifugally driven interchange motions in which cold dense plasma moves outward and is replaced by hotter, more tenuous plasma moving inward (*20*). In the corotating frame, gradient and curvature drifts caused by the magnetic field disperse ions and electrons eastward and westward, respectively, at a rate proportional to their thermal energies. The slope of energy versus time-of-arrival can be used to infer the age of the particles after injection. With this method, we estimated ages in the range 1.5 to tens of hours, indicating that the oldest injection signatures can persist for the order of one planetary rotation, which is comparable to the ages of similar events reported at Jupiter (*19*). The inner boundary of electron-injection signatures (which are the most prominent) is ~4.4 R_S. Consistent with interchange motions of magnetic flux tubes, a few instances of intense plasma acceleration were observed, which may have been caused by low-frequency magnetohydrodynamic (MHD) waves or strong Alfvenic perturbations of the magnetic field ($\Delta B/B > 0.1$) seen at the same time (*21–24*).

As Cassini proceeded deeper into the magnetosphere, the concentrations of O^+ and W^+ relative to H^+ remained near unity or above from ~8 R_S to ~5 R_S, then increased again at C and C′ (Figs. 1 to 3). We estimate that both N^+ and H_3O^+ are present at abundances of ~3% inward as far as 3.4 R_S (at that point the CAPS sensors were turned off as a precaution against degradation during the firing of the Cassini main engine). The N^+ ions, which are low energy (20 to 100 eV) (Fig. 2), cannot be ionized near Titan and transported inward because they would be heated to many keV in the process. We conclude that the N^+ observed inside 8 R_S, although its ultimate source may have been Titan's atmosphere (*25*), must be ionized locally. This could result from neutral nitrogen ejected from Titan that reaches the inner magnetosphere before being ionized (*12*), or ions from Titan that are implanted or adhere to the surfaces of the inner icy satellites or E-ring particles and subsequently are sputtered off (*26*). A possibility is that the nitrogen ions may be indicative of a small abundance of ammonia in these surfaces, an idea that has been proposed to explain morphologic features on Enceladus (*27*).

The inner plasmasphere can be identified with the E ring (~3 to 8 R_S), which is a rich source of water vapor (*28*). Because the ion population there has a low mean energy (Fig. 2C), it is also a region where the relative speeds between neutral gas moving at Keplerian velocities and ion species moving at corotation velocities are low, so that ion-molecule reactions become important (*29*). Our observation of H_3O^+ is interesting as an example of these reactions because it shows that hydronium ions are created in ion-molecule reactions that take place in a water-dominated atmosphere. One source is the reaction $H_2O^+ + H_2O \rightarrow H_3O^+ + OH$, which, in addition to producing the ion, would also contribute to the observed OH torus (*30*). The production of H_3O^+ is similar to processes occurring in the water-rich environment of cometary comas as observed, for example, at comet Halley (*31*). The C and C′ boundaries also mark the point at which the suprathermal electron fluxes drop out (Fig. 2), possibly because of ionizing collisions with the neutral gas cloud associated with the icy satellites and E ring, which is densest at ~5 R_S (*32*).

When CAPS was turned back on at 03:25 UT after the main engine burn, the spacecraft was outbound at 1.65 R_S from the center of Saturn and 18,000 km above the inner part of the B ring. Between 03:37 and 04:09 UT, Cassini was in eclipse behind Saturn; however, the rings were still illuminated from the opposite side of the ring plane on magnetic field lines conjugate to the spacecraft. During this time, we observed a layer of ions (effectively an ionosphere) over the rings (Fig. 4). Based on Langmuir probe measurements, electron densities were $<3 \times 10^6$ m^{-3} (*33*), from which we conclude that the spacecraft very likely was negatively charged by a few volts, which prevented the ELS from entirely measuring the electron velocity distribution. A negative spacecraft potential would also attract positive ions and accelerate them into the IMS. This would improve the chances of measuring atomic or molecular hydrogen ions (corotational energy ~2 eV), which, nonetheless, are not evident (Fig. 4).

Electron count rates are lowest above the B ring, highest over the Cassini division, and intermediate above the A ring; in other words, they vary inversely with ring optical depth (*34*). This inverse correlation suggests that the electrons may originate from photoemission of magnetically conjugate particles in sunlight on the far side of the rings. The peak ion rates began ~5 minutes before the spacecraft reached the Cassini division, whereas the peak electron rates were highest directly over it (Fig. 4, A and B), possibly reflecting the effect of a negative spacecraft potential on electrons. The bulk of the ring ionosphere is made up of $M/Q = 16$ and 32 amu/e ions (Fig. 4C), which we identify as O^+ and O_2^+, respectively (*35*). This finding is consistent with corotation and a temperature of 0.75 eV for both species. Any hydrogen ions present (atomic or molecular) had relative concentrations <3%. After 03:57 UT, the spacecraft turned so that the IMS was no longer pointed in the corotation ram direction, causing ion count rates to drop (Fig. 4B). However, the electron distribution was closer to isotropy in the field-of-view of the ELS, permitting measurements to continue.

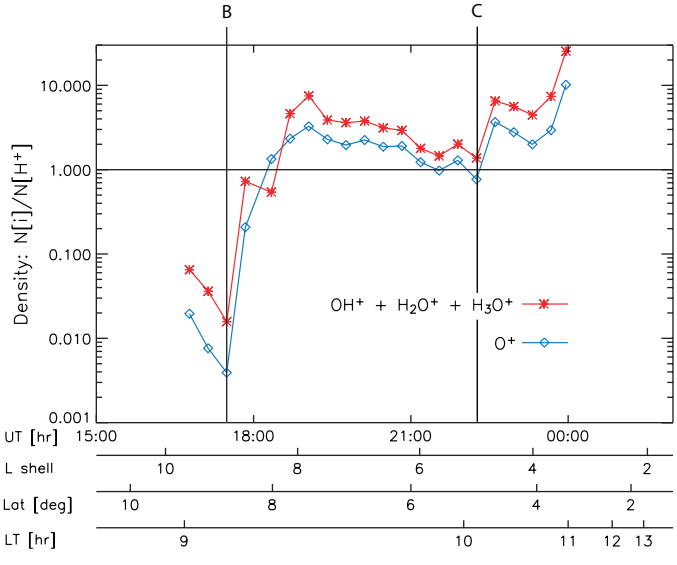

Fig. 3. The concentrations of O^+ and water-group ions are shown relative to H^+ on the inbound leg. Data are 20-min averages calculated by assuming all ions have an isotropic distribution in the spacecraft frame of reference. This assumption is not needed for Fig. 2C. Errors in relative density are estimated to be ±30% for O^+ and OH^+ and ±60% for H_2O^+ and H_3O^+. The L shell is equivalent to the radial distance R_S.

The detection of O_2^+ as a principal ion points to the existence of a layer of molecular oxygen gas over the rings, which we refer to as an atmosphere. Although O_2^+ can originate through photolytic processes in water vapor (*36*), the O_2 atmosphere over the rings, like the atmospheres of Europa and Ganymede, is more likely the result of radiation-induced decomposition of ice (*37*, *38*). In the inner plasmasphere, O_2 can be produced from ice by plasma with energy above a few keV. However, over the rings, energetic plasma fluxes are negligible, leaving production from ice by ultraviolet photons as the primary O_2 source (*39*). Although this is an inefficient process, the O_2 does not stick to the ring particles, whereas O and H_2O and its dissociation fragments stick or react at these temperatures. Therefore, O_2 is the dominant gas-phase species leading to the formation of O_2^+ and O^+ by photoionization in a ratio of ~4:1, which is close to our measurement (Fig. 4C) except for the period 03:39 to 03:43 UT. By using the photoproduction rates of O_2 from ice (*40*) as a lower limit to the source rate, together with photoionization and photodissociation loss rates, we estimate that the O_2 column above the rings is $>2 \times 10^{17}$ m^{-2}. O_2^+ ions that are produced north of the ring plane will oscillate about the magnetic equator, which lies ~2000 km north of the ring plane. These ions are eventually lost to the rings or to molecular collisions in one bounce period, giving an average O_2^+ density of $\sim 3 \times 10^6$ m^{-3}, which is consistent with our measurements. In isolation, photolysis of ice would also produce an H_2 atmosphere over the rings. However, the low concentration of hydrogen ions indicates that the surfaces of the ring particles, together with the ring atmosphere, must be treated as a complete system. For example, processes such as charge exchange and photodissociation of water or H_2 molecules can liberate hydrogen with sufficient energy to remove it from the rings, leaving behind an oxygen-rich atmosphere.

We have observed important features in the plasma distributions, dynamics, and composition of Saturn's magnetosphere that challenge current models. The data taken during Cassini's passage through the inner plasmasphere and its only passage through the inner rings indicate that, although the source material in both regions is mainly water ice, the makeup of the plasma depends critically on ion-molecule chemistry and transport. Thus, the inner plasmasphere, which is rich in water-group ions including H_3O^+, is somewhat analogous to a cometary coma, and the rings' O_2 atmosphere is similar in composition to those of Europa and Ganymede. The presence of low-energy N^+ deep in the magnetosphere points to local sources of nitrogen. The implications of our findings for the cycle of neutral gas and plasma generation and their redistribution are not clear and must await further measurements and modeling. Future orbits (there are 74 remaining) will allow us to substantiate and improve the accuracy of these results.

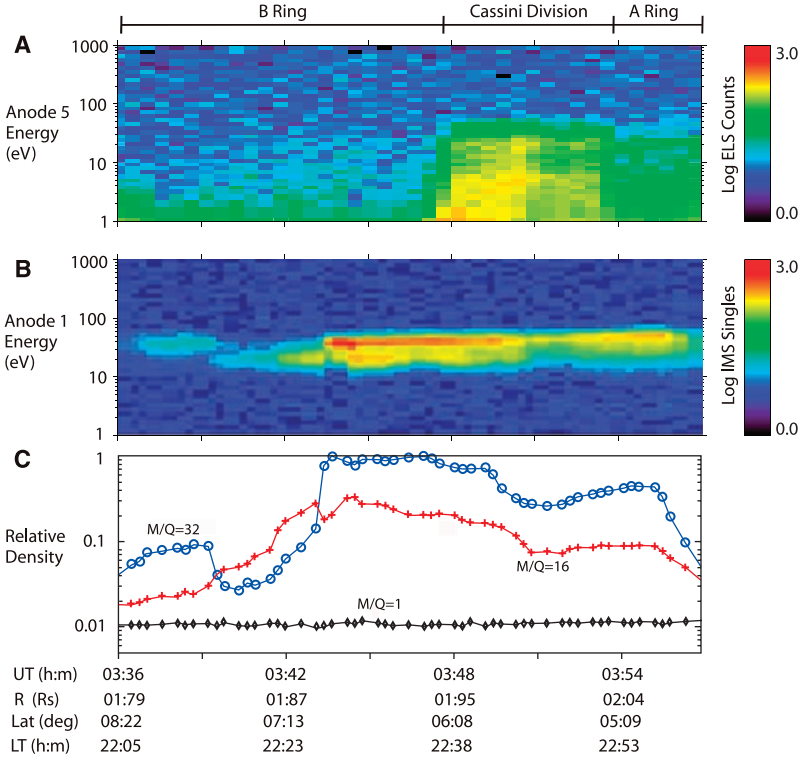

Fig. 4. Color spectrograms and relative ion densities over the A and B rings. (**A**) Electron energy-time spectrogram in the same format as Fig. 1. (**B**) Ion energy-time spectrogram in the same format as Fig. 1. (**C**) Ion density normalized to the maximum density and plotted in arbitrary units. The density was determined from the total IMS ion flux and the assumption of ion corotation. The identification of *M*/*Q* as 16 and 32 ions is consistent with this assumption. Because of the limited IMS high-voltage range during this period, true mass-spectral identification from TOF data is not yet available. The Cassini ring labels correspond to the mapping of magnetic field lines between the spacecraft and the ring plane. At 03:57 UT, the spacecraft began a turn that prevented CAPS from viewing in the direction needed to detect corotating ions. Valid electron measurements extending past 03:57 UT show that the ionosphere extends out to the edge of the A ring.

References and Notes

1. L. A. Frank, B. G. Burek, K. L. Ackerson, K. L. Wolfe, J. D. Mihalov, *J. Geophys. Res.* **85**, 5695 (1980).
2. H. S. Bridge *et al.*, *Science* **212**, 217 (1981).
3. H. S. Bridge *et al.*, *Science* **215**, 563 (1982).
4. E. C. Sittler, K. W. Ogilvie, J. D. Scudder, *J. Geophys. Res.* **88**, 8847 (1983).
5. A. J. Lazarus, R. L. McNutt, *J. Geophys. Res.* **88**, 8831 (1983).
6. J. D. Richardson, E. C. Sittler, *J. Geophys. Res.* **95**, 12019 (1990).
7. S. Maurice *et al.*, *J. Geophys. Res.* **101**, 15211 (1996).
8. J. D. Richardson, *Rev. Geophys.* **36**, 501 (1998).
9. D. T. Young *et al.*, *Space Sci. Rev.* **114**, 1 (2004).
10. The IMS, ELS, and IBS measure particle direction-of-arrival over one hemisphere with resolutions of 8° × 20°, 5° × 20°, and 1.5° × 1.5°, respectively. Two-dimensional energy-angle spectra are measured continuously every 2 s by the ELS, and every 4 s by the IMS. IBS energy spectra are measured every 2 s. Electron distributions are often isotropic, or nearly so, during the period reported here and can be observed by the ELS regardless of spacecraft orientation, which can be highly variable. Ion flux, on the other hand, is often observed to be directional, and our ability to view it depends on spacecraft orientation.
11. Relative to Voyager measurements, CAPS has greatly improved capabilities in three critical areas. (i) The IMS is a true mass spectrometer, not generally dependent on assumptions about ion *E*/*Q* distributions for derivation of ion *M*/*Q*. (ii) Voyager gaps in *E*/*Q* coverage <10 V and 6 to ~30 kV are filled. (iii) Temporal coverage is improved from one 3.8-s energy spectrum taken every 96 s to contiguous spectra taken every 2 s (by the ELS and IBS) or 4 s (by the IMS). One other important difference is that CAPS observations extend to as close as 1.7 R_S over the rings compared with 2.7 R_S for Voyager 2.
12. H. T. Smith, R. E. Johnson, V. I. Shematovich, *Geophys. Res. Lett.* **31**, L16804 (2004).
13. A corotating plasma with the same angular velocity as the planet has an ion energy of $0.5M(R/R_S)^2$ eV, where *M* is ion mass in amu. This formula is used to calculate the corotation curves superimposed on Figs. 1 and 2.
14. A. Nishida, *J. Geophys. Res.* **71**, 5669 (1966).
15. T. W. Hill, A. J. Dessler, F. C. Michel, *Geophys. Res. Lett.* **1**, 3 (1974).
16. J. D. Richardson, *Geophys. Res. Lett.* **22**, 1177 (1995).
17. J. D. Richardson, A. Eviatar, M. A. McGrath, V. M. Vasyliunas, *J. Geophys. Res.* **103**, 20245 (1998).
18. B. H. Mauk, C. I. Meng, *J. Geophys. Res.* **88**, 10011 (1983).
19. B. H. Mauk, D. J. Williams, R. W. McEntire, *Geophys. Res. Lett.* **24**, 2949 (1997).
20. D. H. Pontius Jr., T. W. Hill, M. E. Rassbach, *Geophys. Res. Lett.* **13**, 1097 (1986).
21. M. Dougherty *et al.*, *Science* **307**, 1266 (2005).
22. W. D. Cummings, A. J. Dessler, *J. Geophys. Res.* **72**, 1007 (1967).
23. D. J. Knudsen, M. C. Kelley, J. F. Vickrey, *J. Geophys. Res.* **97**, 77 (1992).
24. A. Hasegawa, K. Mima, *J. Geophys. Res.* **83**, 1117 (1978).
25. A. Eviatar, *J. Geophys. Res.* **89**, 3821 (1984).
26. M. L. Delitsky, A. L. Lane, *J. Geophys. Res.* **107**, 5093 (2002).
27. J. S. Kargel, S. Pozio, *Icarus* **119**, 385 (1996).

28. S. Jurac *et al.*, *Geophys. Res. Lett.* **29**, 2172 (2002).
29. R. E. Johnson *et al.*, *Icarus* **77**, 311 (1989).
30. D. E. Shemansky, P. Matheson, D. T. Hall, H.-Y. Hu, T. M. Tripp, *Nature* **363**, 329 (1993).
31. H. Balsiger *et al.*, *Nature* **321**, 330 (1986).
32. S. Jurac, R. E. Johnson, J. D. Richardson, C. Paranicas, *Planet. Space Sci.* **49**, 319 (2001).
33. D. A. Gurnett *et al.*, *Science* **307**, 1255 (2005).
34. L. W. Esposito *et al.*, in *Saturn*, T. Gehrels, M. S. Edwards, Eds. (Univ. of Arizona Press, Tucson, AZ, 1984), pp. 463–545.
35. This identification was made without time-of-flight (TOF) spectra because at this time, the IMS TOF system was not operating at full voltage and so was out of calibration. Further analysis of the spectra will allow us to positively identify the ion species.
36. W.-I. Ip, *Icarus* **115**, 295 (1995).
37. R. E. Johnson, T. I. Quickenden, P. D. Cooper, A. J. McKinley, C. Freeman, *Astrobiology* **3**, 823 (2003).
38. R. E. Johnson *et al.*, in *Jupiter: The Planet, Satellites, and Magnetosphere*, F. Bagenal, T. Dowling, W. B. McKinnon, Eds. (Cambridge Univ. Press, Cambridge, 2004), pp. 485–512.
39. M. Shi *et al.*, *J. Geophys. Res.* **100**, 26387 (1995).
40. R. E. Johnson, T. I. Quickenden, *J. Geophys. Res.* **102**, 10985 (1997).
41. The CAPS instrument and investigation represent the culmination of 16 years of effort by a team of 170 engineers and scientists at 15 institutions in 6 countries. We wish to thank all team members for their contributions and dedication to the CAPS and Cassini effort. Data reduction and analysis in the United States is supported by NASA/Jet Propulsion Laboratory under contract 1243218 with the Southwest Research Institute. Work at Los Alamos was performed under the auspices of the U.S. Department of Energy. We also wish to thank national funding agencies in Finland, France, Hungary, Norway, and the UK Particle Physics and Astronomy Research Council for their support.

7 October 2004; accepted 10 December 2004
10.1126/science.1106151

REPORT

Cassini Magnetometer Observations During Saturn Orbit Insertion

M. K. Dougherty,[1]* N. Achilleos,[1] N. Andre,[2] C. S. Arridge,[1] A. Balogh,[1] C. Bertucci,[1] M. E. Burton,[3] S. W. H. Cowley,[4] G. Erdos,[5] G. Giampieri,[1] K.-H. Glassmeier,[6] K. K. Khurana,[7] J. Leisner,[7] F. M. Neubauer,[8] C. T. Russell,[7] E. J. Smith,[3] D. J. Southwood,[9] B. T. Tsurutani[3]

Cassini's successful orbit insertion has provided the first examination of Saturn's magnetosphere in 23 years, revealing a dynamic plasma and magnetic environment on short and long time scales. There has been no noticeable change in the internal magnetic field, either in its strength or its near-alignment with the rotation axis. However, the external magnetic field is different compared with past spacecraft observations. The current sheet within the magnetosphere is thinner and more extended, and we observed small diamagnetic cavities and ion cyclotron waves of types that were not reported before.

The first in situ observations from Saturn's magnetosphere in 23 years were obtained during Cassini's Saturn orbit insertion on 30 June 2004. The magnetometer instrument (*1*) (MAG) obtained data on upstream waves, bow shock, magnetosheath, magnetopause, magnetospheric currents, and waves, as well as the planetary magnetic field. These data are consistent with measurements made on earlier missions, provide more detail of some parameters such as the planetary magnetic field, including its possible secular variation, and reveal some features in the external field not previously reported.

The solar wind controls the size of the magnetosphere and the dynamics of its outer reaches. Because the solar wind speed is supersonic, the deflection of the solar wind occurs via a standing bow shock that compresses and heats the solar wind, forming the magnetosheath. The inner edge of the magnetosheath, the magnetopause, marks the outer boundary of the region controlled by the planetary magnetic field. Saturn's bow shock is of intrinsic interest because it is expected to be much stronger than that of Earth. The magnetopause is important because it controls the coupling of the solar wind flow to the magnetosphere, principally, we expect, through the process known as reconnection (*2*). The locations of both boundaries are determined by the dynamic pressure of the solar wind and the combined plasma and magnetic pressure of the magnetosphere.

The boundaries were observed to be very dynamic. We measured a total of 17 bow shock and 7 magnetopause crossings (Fig. 1) on the inbound and outbound passages. Bow shock crossings were identified by abrupt increases in the magnetic field magnitude where the solar wind was compressed and decelerated. As Cassini approached Saturn near 08:00 local time (LT), it crossed the bow shock on seven separate occasions, starting at 09:45 universal time (UT) on 27 June 2004 at a distance of $49.15R_S$ [$1\ R_S = 60{,}268$ km (*3*)]. The last inbound bow shock crossing occurred at 05:38:30 UT on 28 June 2004 at a distance of $40.5R_S$. At least 10 crossings of the bow shock were observed on the outbound leg in the magnetometer data, with the earliest bow shock crossing observed on 7 July 2004 at a radial distance range of $56R_S$ and the final bow shock crossing occurring on 14 July 2004 at $85R_S$. Saturn's bow shock is expected to be a strong quasi-perpendicular shock. A large overshoot in the magnetic field magnitude is a consistent feature of the shock crossings and is a typical feature of supercritical planetary bow shocks (*4*). These observations afford us the opportunity to study bow shocks at high Mach numbers, which are rarely observed on Earth. Indeed, the Mach number can be inferred from the amplitude of the overshoot $\delta B/B_0$ (*5*). The average value for the bow shocks observed is ~1.5, consistent with a fast magnetosonic Mach number as high as 8.

On the Saturnian side of the bow shock lies the magnetosheath, where the magnetic field is very turbulent and dominated by wave activity. The entrance into the magnetosphere was preceded by multiple crossings of the magnetopause on 28 June and 29 June 2004. On the outbound pass, the spacecraft exited the magnetosphere near 05:00 LT. The first excursions into the inner magnetosheath were characterized by the presence of mirror mode structures. The multiple crossings of these plasma boundaries reveal the dynamic character of Saturn's outer magnetosphere in response to variations in the solar wind ram pressure.

Before the Cassini arrival at Saturn, there had been three previous flybys: Pioneer 11 (*6*) and Voyager 1 and 2 (*7*, *8*). The spatial coverage of these flybys was limited, with the inbound trajectories all being in the noon sector and outbound Pioneer 11 and Voyager 1

[1]Blackett Laboratory, Imperial College London, SW7 2AZ, UK. [2]CESR, 31028 Toulouse, France. [3]Jet Propulsion Laboratory, California Institute of Technology, Pasadena, CA 91109, USA. [4]Department of Physics and Astronomy, Leicester University, Leicester, LE1 7RH, UK. [5]KFKI Research Institute for Particle and Nuclear Physics, H-1525 Budapest, Hungary. [6]Technische Universitat Braunschweig, D-38106 Braunschweig, Germany. [7]University of California Los Angeles Institute of Geophysics and Planetary Physics, Los Angeles, CA 90024, USA. [8]Institute for Geophysics and Meterology, Köln University, 50923 Köln, Germany. [9]European Space Agency, 75738 Paris, France.

*To whom correspondence should be addressed. E-mail: m.dougherty@imperial.ac.uk